Comparing Simulated Electrocardiograms of Different Stages of Acute Cardiac Ischemia

Mathias Wilhelms, Olaf Dössel, and Gunnar Seemann

Institute of Biomedical Engineering, Karlsruhe Institute of Technology (KIT)
Kaiserstr. 12, 76131 Karlsruhe, Germany
publications@ibt.kit.edu
http://www.ibt.kit.edu

Abstract. Diagnosis of acute cardiac ischemia depends on characteristic shifts of the ST segment. The transmural extent of the ischemic region and the temporal stage of ischemia have an impact on these changes. In this work, computer simulations of realistic ventricles with different transmural extent of the ischemic region were carried out. Furthermore, three stages within the first half hour after the occlusion of the distal left anterior descending coronary artery were regarded. The transmembrane voltage distributions and the corresponding body surface ECGs were calculated. It was observed how the electrophysiological properties worsen in the course of ischemia, so that almost no excitation was initiated in the central ischemic zone 30 minutes after the occlusion. In addition to these temporal effects, also the transmural extent of the ischemic region had an impact on the direction and intensity of the ST segment shift.

Keywords: Cardiac Ischemia, Phase 1b, Electrocardiogram, Mathematical Modeling, ST Segment Shift.

1 Motivation

The occlusion of a coronary artery due to e.g. atherosclerosis leads to a deficient blood supply of the heart muscle. This pathology, which is termed acute cardiac ischemia, leads to lethal heart failure or severe ventricular arrhythmias in many cases. During the first thirty minutes after the occlusion, two different phases of arrhythmias can be identified [1]. The so-called phase 1a peaks between 2 and 10 minutes and phase 1b between 20 and 30 minutes after the onset of ischemia [2].

In phase 1a, mainly three ischemia effects can be observed: hyperkalemia, acidosis and hypoxia. Due to this, the conduction velocity (CV), the action potential (AP) amplitude and duration are reduced and the resting transmembrane voltage is increased [3]. These time-dependent electrophysiological changes are classified with increasing ischemia: 5 to 7 minutes after the occlusion, stage 1 (S1) is reached and stage 2 (S2) after 10 to 12 minutes [4].

Phase 1b is characterized by cellular uncoupling, which means that the gap junctional conductance decreases. In addition, the extracellular potassium concentration ($[K^+]_o$) and the intracellular calcium concentration ($[Ca^{2+}]_i$) increase, which also favors initiation of arrhythmias [1].

D.N. Metaxas and L. Axel (Eds.): FIMH 2011, LNCS 6666, pp. 11–19, 2011.

Depending on the degree of the occlusion and the occlusion site, ischemia effects vary spatially. They appear in the subendocardium at first, which is called *subendocardial ischemia*. Then, they spread transmurally towards the subepicardium, if the occlusion of the artery continues for longer periods (*transmural ischemia*) [5]. However, ischemia effects are stronger in the subepicardial tissue, since, inter alia, the sensitivity of the ATP regulated potassium channels is higher there [6].

The diagnosis of cardiac ischemia is based on changes in the electrocardiogram (ECG), as for example shifts of the ST segment. Depending on the transmural extent of the ischemic region, ST segment elevation or depression can be observed in leads close to the ischemic region. The reason for these deviations is the direction of injury currents, which flow from healthy or less injured towards ischemic tissue [7]. Nevertheless, the exact underlying mechanisms responsible for these ECG alterations and the dynamic changes during the first thirty minutes of ischemia are not completely understood. In order to improve the early diagnosis of acute cardiac ischemia, computer simulations are a helpful tool. For this purpose, the electrocardiograms of different ischemic stages of the heart with varying transmural extent of the ischemic region were investigated *in silico* in this work.

2 Methods and Materials

Aiming at simulation of the impact of acute cardiac ischemia on electrocardiograms, a ventricular cell model was modified to reproduce ischemia effects at different stages. Then, the transmembrane voltage distribution was computed in a realistic model of human ventricles with varying transmural extent of the ischemic region. Finally, the corresponding body surface potential maps (BSPMs) were calculated and the ECGs were extracted.

2.1 Modeling Ischemic Myocytes

The simulation of acute cardiac ischemia was based on the ventricular cell model published in 2006 by ten Tusscher et al. [8]. The model provides an electrophysiological description of endocardial, midmyocardial and epicardial myocytes. Furthermore, the model was modified according to Weiss et al. [3] in order to simulate phase 1a ischemia effects, which are hyperkalemia, acidosis and hypoxia. For both stages S1 and S2, different parameter sets were used. The formulation of the ATP sensitive potassium channel was modified, so that the current was inhibited at healthy ADP concentrations. For this purpose, the half-maximum inhibition constant was adjusted ($K_m = (-151.0919+75.5379 \cdot [ADP]_i^{0.256}) \cdot K_{m,factor}$). As a consequence, the ADP concentrations at stage 1 and phase 1b were adapted (compare Table 1).

For the simulation of phase 1b cardiac ischemia, even more parameters, i.e. the maximal conductances of I_{NaK}, I_{NaCa}, I_{up} and I_{rel} (P_{NaK}, k_{NaCa}, V_{maxup} and V_{rel}), were modified according to Pollard and coworkers [9]. In this way, changes of the intracellular calcium handling, pumps and exchangers were considered.

Table 1. Cell model parameters at different stages of acute ischemia in the central ischemic zone according to [3,9,10,11]. g_{Na} and $g_{Ca,L}$ are the sodium and calcium channel conductivities, $dV_{m,Na}$ is the voltage shift of sodium channels, and $[ATP]_i$ and $[ADP]_i$ are the intracellular concentrations of ATP and ADP

Cell model parameter		control (0 min)	stage 1 (5 min)	stage 2 (10 min)	phase 1b (20–30 min)
$[K^+]_o$	(mmol/l)	5.4	8.7	12.5	15.0
g_{Na},$g_{Ca,L}$	(%)	100	87.5	75	50
$dV_{m,Na}$	(mV)	0	1.7	3.4	3.4
$[ATP]_i$	(mmol/l)	6.8	5.7	4.6	3.8
$[ADP]_i$	(μmol/l)	15	87.5	99	101.5
P_{NaK}	(%)	100	100	100	30
k_{NaCa}	(%)	100	100	100	20
V_{maxup}	(%)	100	100	100	90
V_{rel}	(%)	100	100	100	5

Since the background calcium current I_{bCa} is small compared to other currents and the calcium sensitive nonselective cation current $I_{ns,Ca}$ is not implemented in this model, the metabolic changes of these currents were neglected here. An overview of the modified cell model parameters is given in Table 1.

2.2 Modeling Heterogeneous Excitation Propagation

The anatomical model of the ventricles used in this work was derived from MR images of a healthy volunteer. This dataset was interpolated to an isotropic cubic voxel size of 0.4 mm. The longitudinal intracellular conductivity, which was scaled through the ventricular wall as described in [12], was on average 0.26 S/m resulting in a conduction velocity of approximately 0.65 m/s. The anisotropy factor was set to 2.6. The cardiac fiber orientation was modeled using a rule-based method as in [12].

Different electrophysiological heterogeneities were considered for the simulations shown in this work. For this purpose, the ventricular wall was divided into 20% epicardial, 40% midmyocardial and 40% endocardial tissue [12]. As already included in the cell model of ten Tusscher et al. [8], transmurally differing values for the conductivities of the slow delayed rectifier potassium channel (g_{Ks}), the transient outward potassium channel (g_{to}) and the corresponding channel kinetics were used. Furthermore, an apico-basal gradient of g_{Ks} resulting in a two times larger value at the apex (compare Fig. 1) allowed the simulation of a T-wave comparable to the measurements of the healthy volunteer.

The effects of cardiac ischemia also varied spatially. The half-maximum inhibition constant K_m of the ATP sensitive potassium channel was largest in epicardial and smallest in endocardial tissue. This ensured the transmurally differing sensitivity of this channel to changes of $[ATP]_i$ and $[ADP]_i$ [3]. The ischemic region was described by the so-called zone factor (ZF), which described the regional influence of the occluded coronary artery (see also Fig. 1). Its values ranged from 0 (healthy tissue) to 1 (central ischemic zone, CIZ), intermediate

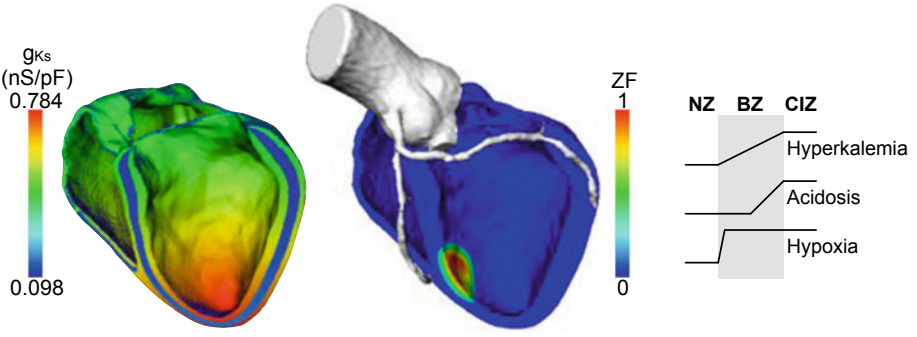

Fig. 1. Ventricular model showing transmural and apico-basal heterogeneity of g_{Ks} (*left*) and zone factor (ZF) with a subendocardial ischemic region and coronary arteries (*middle*). Border zones of different ischemia effects (*right*).

values described the border zone (BZ). The different ischemia effects developed unequally across the BZ, which had a thickness of 5.6 mm in this example. As in [10], the effects of hyperkalemia underwent a linear course from the beginning to the end of the BZ, whereas the impact of acidosis began at 50% of the BZ. However, the effects of hypoxia were fully present after 10% of the BZ (compare Fig. 1). In order to model cellular uncoupling during phase 1b, the intracellular conductivity was linearly decreased from healthy tissue (100%) to the CIZ (12.5%) [11]. The ischemic regions were modeled as ellipsoids with their centers on the endocardial surface. In order to investigate the impact of the transmural extent of the ischemic region on the ECG, a subendocardial, an intermediate and a transmural ischemic region were created. The total size of the ischemic region varied between 2.9% (subendocardial ischemia) and 5.6% (transmural ischemia) of the volume of the left ventricle. The size of the endocardial surface, which was affected by cardiac ischemia, was equal in all three cases. The ischemic region was located at the distal left anterior descending coronary artery (see Fig. 1).

Cardiac ischemia effects at different stages were initialized in a single-cell environment. Afterwards, simulation of cardiac excitation propagation was carried out using the parallel monodomain solver *acCELLerate* [13] with a time step of 20 μs in the 3D ventricular model. For this purpose, an endocardial stimulation profile as in [12] mimicking the His-Purkinje conduction system, which describes the time instant and location of ventricular stimulation, was used.

2.3 Calculation of Body Surface Electrocardiograms

The simulated BSPMs were obtained by solution of the forward problem of electrocardiography. For this purpose, the previously calculated transmembrane voltages in the heart model were interpolated onto a high resolution tetrahedron model of the torso ($\approx$ 1.3 million nodes). This torso contained the following tissue types in addition to the heart: blood, lungs, fat, skeletal muscle, intestine, kidneys, liver and spleen. After the interpolation, the bidomain equations were used to determine the corresponding body surface potentials with inhomogeneous

tissue conductivities as described in [12]. As in the ventricular simulations, the intracellular conductivity of the heart was linearly decreased to 12.5% across the BZ in the ischemic region in case of phase 1b ischemia.

3 Results

3.1 Cell Simulations

The cell model was initialized, so that the effects of the different stages of acute ischemia were fully present. Since the changes due to cardiac ischemia were most prominent in epicardial myocytes, only the results of this cell type are shown here. The APs at different stages of cardiac ischemia are depicted in Fig. 2.

The changes of the action potential parameters were also consequently greatest in epicardial cells (see Table 2). The APD_{90} (measured at 90% repolarization) gradually decreased to 18.2% of the control value after 30 min of cardiac ischemia. The resting transmembrane voltage $V_{m,rest}$ increased and the peak transmembrane voltage $V_{m,max}$ decreased in the course of ischemia.

3.2 Tissue Simulations

Altogether, ten simulations using the 3D ventricular model were carried out: one control case and three setups with different transmural extent of the ischemic

Table 2. Action potential parameters of epicardial myocytes at different stages of acute cardiac ischemia

Action potential parameter		control (0 min)	stage 1 (5 min)	stage 2 (10 min)	phase 1b (20–30 min)
APD_{90}	(ms)	309.1	116.5	72.1	56.3
$V_{m,rest}$	(mV)	-85.6	-73.6	-64.3	-58.1
$V_{m,max}$	(mV)	38.4	34.9	18.8	16.5

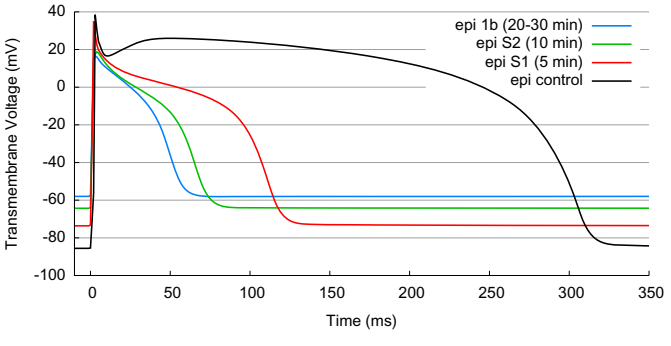

Fig. 2. Action potentials of epicardial myocytes at different stages of acute ischemia

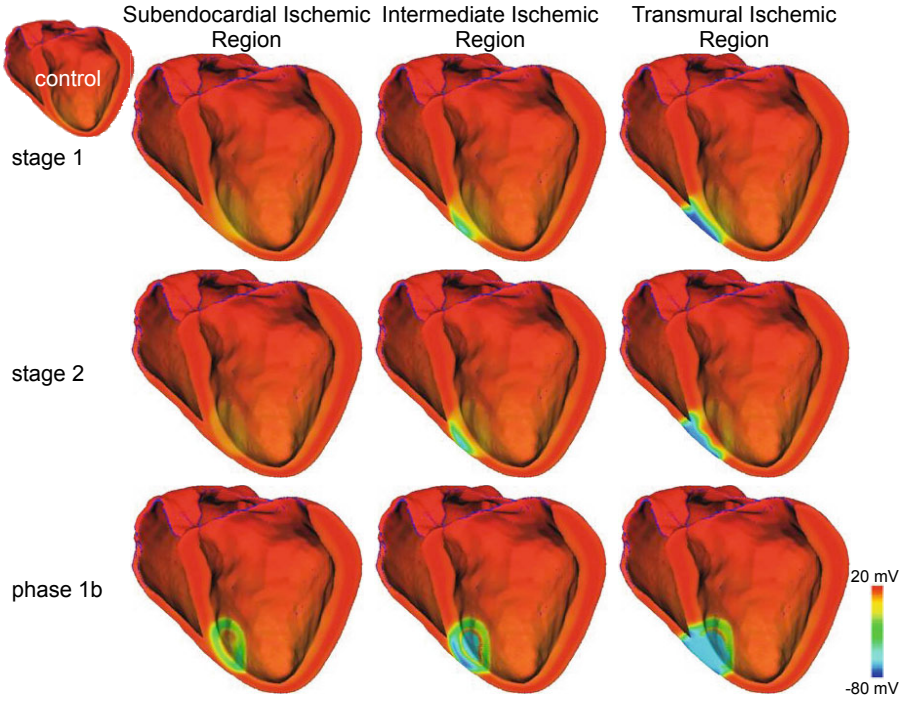

Fig. 3. Transmembrane voltages of different ischemia setups at $t = 200$ ms. The transmural extent of the ischemic region and the stage of ischemia were varied.

region at three ischemia stages each. The resulting transmembrane voltage distributions at $t = 200$ ms after beginning of a normal sinus beat are shown in Fig. 3. The corresponding ECGs, which resulted from these simulations, are plotted in Fig. 4. Since lead V_4 was closest to the ischemic region simulated in this work, the changes due to cardiac ischemia were most prominent in this lead.

In the control case, the ventricles were completely in the plateau phase of the action potential at 200 ms resulting in a nearly zero baseline in lead V_4. During cardiac ischemia, this excitation pattern was changed. In case of subendocardial ischemia, only short APs with low amplitude were initiated in the ischemic region. The ischemia effects intensified with increasing ischemia stage. Since the injury current was flowing from healthy epicardial towards injured endocardial tissue, a pronounced ST segment depression could be observed during phase 1b.

The transmural extent of the ischemic region was slightly increased in the intermediate ischemic region setup. During the first ten minutes, ischemia effects were more pronounced in the midmyocardial and epicardial tissue, which resulted in a slight elevation of the ST segment there. In phase 1b, no excitation was initiated in the endocardial CIZ, whereas the midmyocardial and epicardial BZ were activated. This caused nearly a ST segment depression in the later ischemia stage.

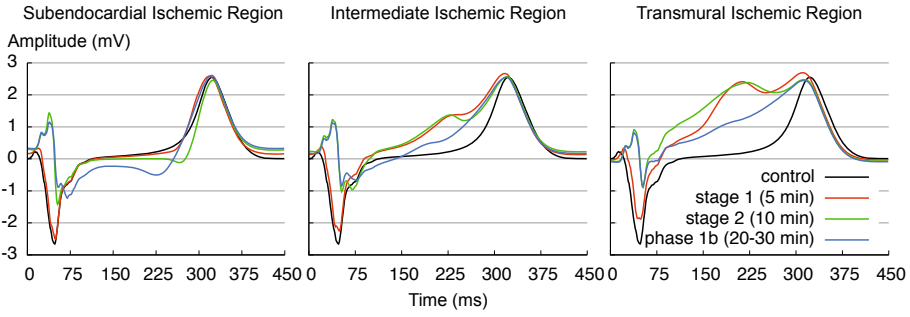

Fig. 4. ECGs (chest lead V_4) of three ischemia cases at different ischemia stages

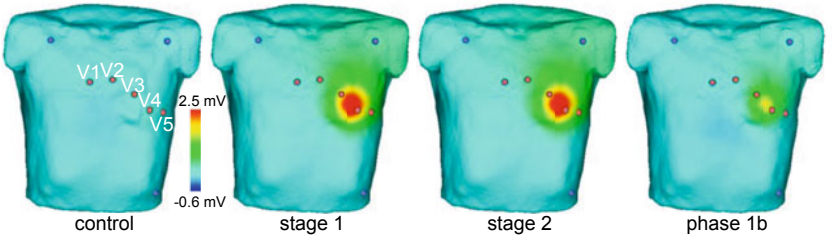

Fig. 5. BSPMs of the transmural ischemia case at $t = 200$ ms at different stages of acute cardiac ischemia

In transmural ischemia, the CIZ of the ischemic region spanned the entire ventricular wall. However, a conduction block was only visible in the epicardium at stage 1 and stage 2. In the endocardium, a delayed activation could be observed. This led to a pronounced elevation of the body surface potential (compare Fig. 5), since the injury current was directed from the less injured endocardium towards the more affected epicardium. During phase 1b, there was also a conduction block in the endocardium. Consequently, the body surface potential was only slightly elevated close to the ischemic region. Next to this area of elevation, the potential was similar to that of the control case.

4 Discussion and Conclusions

In clinical practice, the early diagnosis of cardiac ischemia is based on shifts of the ST segment. In this *in silico* study, we showed that the changes in the ECG depend not only on the transmural extent of the ischemic region, but also on the stage of acute ischemia. Other groups as e.g. [9,10,11] also investigated phase 1b of cardiac ischemia. However, the corresponding body surface ECGs and the differences between several acute ischemia stages were not investigated there.

The effects of cardiac ischemia worsened in the first thirty minutes. On the cellular level, the electrophysiological properties, as e.g. the APD or the AP amplitude, changed gradually. Furthermore, the intracellular conductivity was reduced in the ischemic region during phase 1b. As a consequence, almost no excitation was initiated in the CIZ at this stage. As a result, the ST segment depression was more pronounced in the subendocardial ischemia case and also in the intermediate ischemia case, a ST segment depression can be seen. In the transmural ischemia case, the difference between endocardial and epicardial ischemic tissue decreases during phase 1b compared to the earlier stages. Consequently, ST segment elevation is less pronounced after 20 to 30 minutes. Similar observations have been made in animal experiments [14,15], in which the ST segment elevation decreased at ca. 30 minutes. However, the authors concluded that this could be explained by transitory improvement of the electrophysiological properties of ischemic cells due to a plateau phase of $[K^+]_o$ accumulation. However, lack of experimental data, i.e. human body surface ECGs of the first 30 minutes of cardiac ischemia, do not allow appropriate verification of the findings of these simulations.

The exemplary ischemic region presented in this work shows that the diagnosis of cardiac ischemia based on ST segment shifts can be very difficult. In addition to the transmural extent of the ischemic region, also the temporal stage of ischemia has an impact on the ECG and the direction of the ST segment shift. Some ischemia cases, as e.g. the subendocardial ischemia at stage 1 or stage 2, can hardly be identified in the ECG. As a consequence, early diagnosis of cardiac ischemia should not only rely on 12-lead ECGs. Instead, biomarkers as CK-MB or troponin or multichannel ECG systems should be more emphasized.

In general, the monodomain model is sufficient for the simulation of cardiac excitation propagation and body surface potentials using a high resolution forward model [16]. However, anisotropy ratio may be changed during phase 1b ischemia, which would require use of the bidomain model. As in [9], the model of cardiac ischemia used in this work only indirectly simulates metabolic effects as the inhibition of the Na^+-K^+ pump in order to reduce model complexity. However, detailed metabolic models as in [17] allow more realistic simulations of ischemia effects. Furthermore, a diffusion model of the blood flow in the coronary arteries would create more realistic ischemic regions. Another aspect that should be mentioned is that the spatial resolution of 0.4 mm was a compromise between computing time and accuracy, since the calculation of a single heart beat (450 ms) took approximately 8.5 h on 16 cores. In future simulations, a higher resolution of 0.2 mm will be used. In addition, more simulations with different occlusion sites and varying ischemia size should be carried out in the future.

Acknowledgments

This work has been partially funded within the framework of the nationwide "Initiative for Excellence" from the Karlsruhe Institute of Technology (KIT).

References

1. Carmeliet, E.: Cardiac ionic currents and acute ischemia: from channels to arrhythmias. Physiol. Rev. 79, 917–1017 (1999)
2. Cascio, W., Yang, H., Muller-Borer, B., Johnson, T.: Ischemia-induced arrhythmia: the role of connexins, gap junctions, and attendant changes in impulse propagation. J. Electrocardiol 38, 55–59 (2005)
3. Weiss, D., Ifland, M., Sachse, F.B., Seemann, G., Dössel, O.: Modeling of cardiac ischemia in human myocytes and tissue including spatiotemporal electrophysiological variations. Biomed. Tech. 54, 107–125 (2009)
4. Rodríguez, B., Tice, B., Eason, J., Aguel, F., Ferrero, J., Trayanova, N.: Effect of acute global ischemia on the upper limit of vulnerability: a simulation study. Am. J. Physiol-Heart C 286, 2078–2088 (2004)
5. Colonna, P., Cadeddu, C., Montisci, R., Chen, L., Meloni, L., Iliceto, S.: Transmural heterogeneity of myocardial contraction and ischemia. Diagnosis and clinical implications. Ital Heart J. 1, 174–183 (2000)
6. Furukawa, T., Kimura, S., Furukawa, N., Bassett, A., Myerburg, R.: Role of cardiac ATP-regulated potassium channels in differential responses of endocardial and epicardial cells to ischemia. Circ. Res. 68, 1693–1702 (1991)
7. Foster, D.: Ischemia and Anginal Syndromes. In: Twelve-lead Electrocardiography: Theory and Interpretation. Springer, Heidelberg (2007)
8. ten Tusscher, K., Panfilov, A.: Alternans and spiral breakup in a human ventricular tissue model. Am. J. Physiol-Heart C 291, H1088–H1100 (2006)
9. Pollard, A., Cascio, W., Fast, V., Knisley, S.: Modulation of triggered activity by uncoupling in the ischemic border. A model study with phase 1b-like conditions. Cardiovasc Res. 56, 381–392 (2002)
10. Jie, X., Trayanova, N.: Mechanisms for initiation of reentry in acute regional ischemia phase 1b. Heart Rhythm 7, 379–386 (2010)
11. Ramirez, E., Saiz, J., Trenor, B., Ferrero, J., Molto, G., Hernandez, V.: Influence of 1b ischemic ventricular tissue on the automaticity of purkinje fibers: A simulation study. In: Computers in Cardiology, pp. 617–620 (2007)
12. Keller, D.U.J., Weber, F.M., Seemann, G., Dössel, O.: Ranking the influence of tissue conductivities on forward-calculated ECGs. IEEE Transactions on Biomedical Engineering 57, 1568–1576 (2010)
13. `www.ibt.kit.edu/acCELLerate.php` Cardiac Electrophysiology and Tension Development Software
14. Kleber, A., Janse, M., van Capelle, F., Durrer, D.: Mechanism and time course of S-T and T-Q segment changes during acute regional myocardial ischemia in the pig heart determined by extracellular and intracellular recordings. Circ. Res. 42, 603–613 (1978)
15. Cinca, J., Warren, M., Carreno, A., Tresanchez, M., Armadans, L., Gomez, P., Soler-Soler, J.: Changes in myocardial electrical impedance induced by coronary artery occlusion in pigs with and without preconditioning: correlation with local ST-segment potential and ventricular arrhythmias. Circ. 96, 3079–3086 (1997)
16. Potse, M., Dubé, B., Richter, J., Vinet, A., Gulrajani, R.: A comparison of monodomain and bidomain reaction-diffusion models for action potential propagation in the human heart. IEEE Trans. Biomed. Eng. 53, 2425–2435 (2006)
17. Terkildsen, J., Crampin, E., Smith, N.: The balance between inactivation and activation of the Na^+-K^+ pump underlies the triphasic accumulation of extracellular K^+ during myocardial ischemia. Am. J. Physiol. 293, H3036–H3045 (2007)